STANDARD MODEL RESULTS OF CMS AT 13 TeV*

Muhammad Ahmad

on behalf of the CMS Collaboration

Institute of High Energy Physics, Chinese Academy of Sciences, Beijing, China

(Received May 4, 2016)

The most recent results of Standard Model physics using 13 TeV proton–proton collisions data recorded by CMS detector during the LHC Run 2 are reviewed. This overview includes studies of several results of Forward and Small-x QCD physics, B physics and Quarkonia, Standard Model physics and Top physics. The outlined results are compared to the corresponding theoretical predictions and no significant deviation is observed.

DOI:10.5506/APhysPolB.47.1365

1. Introduction

Standard Model (SM) results from CMS using the LHC Run 2 data have provided us a possibility to perform extensive tests of the electroweak and strong interactions. These measurements are made with the data collected by CMS in the 2015 run, corresponding to an integrated luminosity up to 2.5 fb^{-1} with a bunch spacing of 25 and 50 ns.

2. Forward and Small-x QCD physics results

2.1. Pseudorapidity distributions of charged hadrons and two-particle correlations (the "ridge")

The CMS Collaboration has performed the measurement of pseudorapidity distribution of charged hadrons in pp collisions at $\sqrt{s} = 13$ TeV, at zero magnetic field [1], to test perturbative and nonperturbative quantum chromodynamics (QCD) phenomena, such as saturation of parton densities, multiparton interactions, parton hadronization, and soft diffractive scattering. The center-of-mass energy dependence of $\mathrm{d}N_{\mathrm{ch}}/\mathrm{d}\eta$ is shown in Fig. 1. For comparison with the $\sqrt{s} = 13$ TeV, results obtained at lower energies

* Presented at the Cracow Epiphany Conference on the Physics in LHC Run 2, Kraków, Poland, January 7–9, 2016.

(ISR, UA5, PHOBOS, and ALICE) are also plotted. The PYTHIA 8 and EPOS LHC event generators globally reproduce the collision-energy dependence of hadron production in inelastic pp collisions.

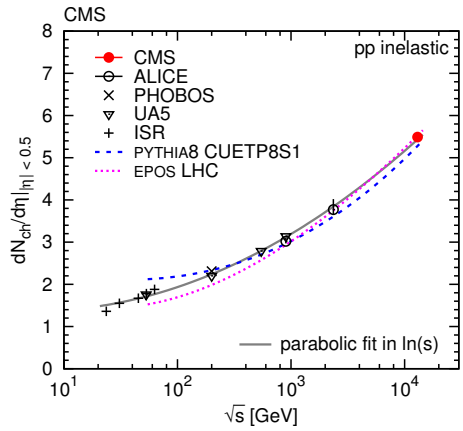

Fig. 1. Center-of-mass energy dependence of $\mathrm{d}N_{\mathrm{ch}}/\mathrm{d}\eta_{|\eta|<0.5}$ including ISR, UA5, PHOBOS, and ALICE data. The solid curve shows a second-order polynomial in $\ln(s)$ fit to the data points, including the new result at $\sqrt{s} = 13$ TeV. The dashed and dotted curves show the PYTHIA 8 CUETP8S1 and EPOS LHC predictions, respectively.

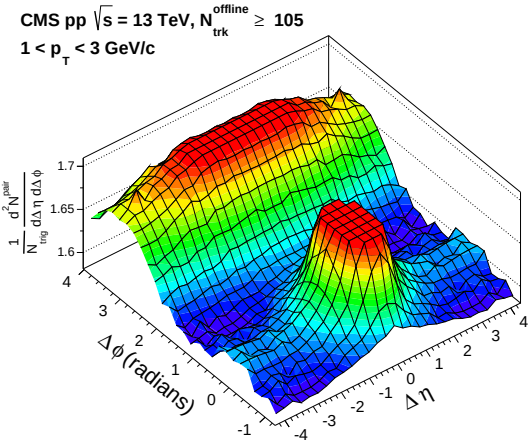

Fig. 2. The 2D $(\Delta\eta, \Delta\phi)$ two-particle correlation functions in pp collisions at $\sqrt{s} = 13$ TeV for pairs of charged particles both in the range of $1 < p_{\mathrm{T}} < 3$ GeV/c. Results are shown for a high-multiplicity sample ($N_{\mathrm{trk}}^{\mathrm{offline}} \geq 105$). The sharp peaks from jet correlations around $(\Delta\eta, \Delta\phi) = (0, 0)$ are truncated to better illustrate the long-range correlations.

The two-dimensional (2D) $\Delta\eta\Delta\phi$ two-particle correlation functions for events with high multiplicities are shown in Fig. 2, for pairs of charged particles both in the range of $1 < p_{\mathrm{T}} < 3$ GeV/c produced in pp collisions at a center-of-mass energy of 13 TeV. The correlations are studied over a broad range of pseudorapidity ($|\eta| < 2.4$) and over the full azimuth (ϕ) as a function of charged particle multiplicity and transverse momentum (p_{T}) [2]. No such long-range (large $\Delta\eta$ small $\Delta\phi$) correlations were expected before their observation in pp collisions at $\sqrt{s} = 7$ TeV data recorded in 2011.

2.2. Underlying event

We have also performed measurement of the underlying event (UE) activity in proton–proton collisions at the center-of-mass energy of 13 TeV with the CMS experiment at the LHC [3], using leading charged-particles as well as leading charged-particle jets as reference objects. Average particle and energy densities are calculated in the transverse region and measured as a function of the p_{T} of the leading charged-particle as well as of the leading charged-particles jet. All charged particles with $p_{\mathrm{T}} \geq 0.5$ GeV and $|\eta| < 2.0$ are used to calculate the UE activity as shown in Fig. 3. Measured distributions are corrected for the detector effects and the selection efficiencies. The corrected distributions are compared with several theory predictions and Monash tune of PYTHIA 8 is found to be in best agreement with the measurements.

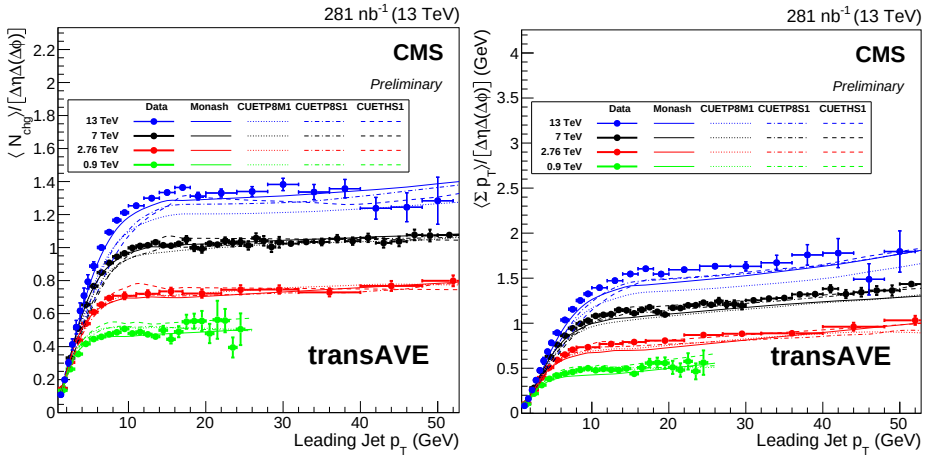

Fig. 3. Comparisons of corrected transAVE particle densities (left), energy densities (right) with various simulations at $\sqrt{s} = 0.9$, 2.76, 7, and 13 TeV as a function of $p_{\mathrm{T}}^{\mathrm{jet}}$.

3. B physics results

3.1. B^+ production cross section

The B^+ meson differential cross sections, as a function of transverse momentum and rapidity, are measured in pp collisions at center-of-mass energy $\sqrt{s} = 13$ TeV, on the basis of a data sample collected by the CMS experiment, corresponding to an integrated luminosity of 50.8 pb^{-1} [4]. The measurement uses the exclusive decay channel $B^+ \to J/\psi K^+$, with the J/ψ decaying to a pair of muons. The results are compared with theory calculations and with measurements made at 7 TeV as shown in Fig. 4. The measured B^+ meson differential cross sections as a function of p_{T}^B for $|y^B| < 2.4$ and as a function of y^B for $10 < p_{\mathrm{T}}^B < 100$ GeV show a reasonable agreement, both in terms of shape and of normalization, with FONNL calculations and with the results obtained with the PYTHIA event generator.

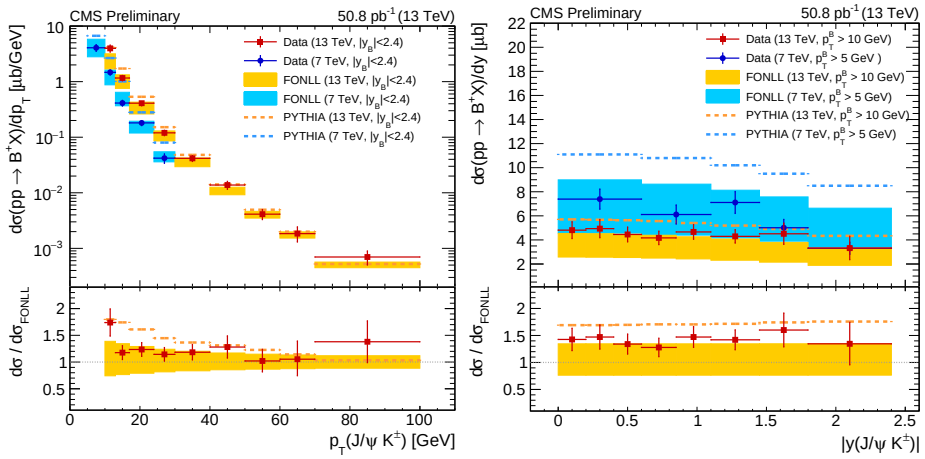

Fig. 4. Differential cross sections $\mathrm{d}\sigma/\mathrm{d}p_{\mathrm{T}}^B$ for $|y^B| < 2.4$ (left) and $\mathrm{d}\sigma/\mathrm{d}y^B$ for $10 < p_{\mathrm{T}} < 100$ GeV (right), for B^+ production in pp collisions at $\sqrt{s} = 13$ TeV.

4. Standard Model physics results

4.1. W/Z production cross section

A measurement of total inclusive and fiducial W and Z boson production cross sections in pp collisions at $\sqrt{s} = 13$ TeV is also performed [5]. Electron and muon final states are studied in a data sample collected with the CMS detector corresponding to an integrated luminosity of up to 43 ± 2 pb^{-1}. The theoretical predictions of cross sections and cross-section ratios are computed at NNLO for five PDF sets. A summary of total and fiducial inclusive W^+,

W^-, W, and Z production cross-sections times branching fractions, W^+, W^-, and W to Z and W^+ to W^- ratios, and their theoretical predictions are shown in Fig. 5. The total uncertainties are splitted into stat., syst. and lumi. uncertainties. The measured values agree with next-to-next-to-leading-order QCD cross-section calculations.

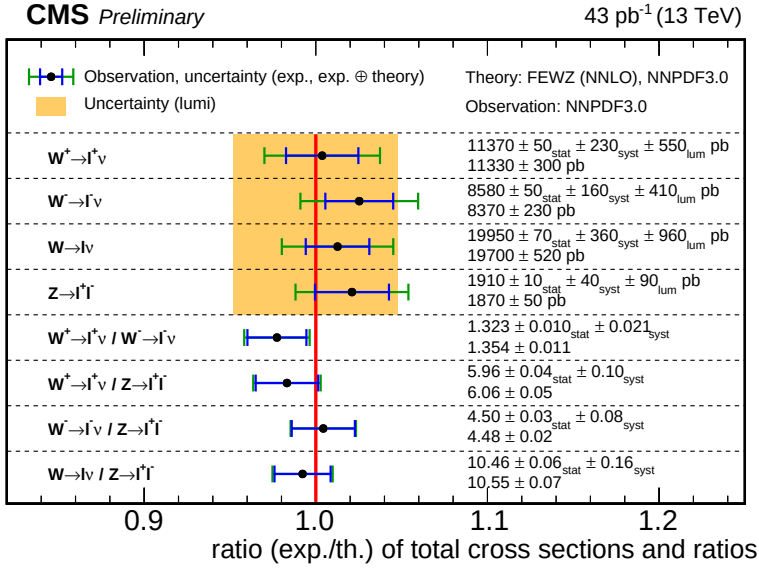

Fig. 5. Summary of total inclusive W^+, W^-, W, and Z production cross-sections times branching fractions, W to Z and W^+ to W^- ratios, and their theoretical predictions. The shaded box indicates the uncertainties in the luminosity measurement. The inner error bars represents the experimental uncertainties, while outer error bars also include the uncertainties in the theoretical predictions. The individual measurements and theoretical predictions are given numerically on the right.

4.2. ZZ/WZ production cross section

We also present measurements of fiducial and total cross sections of ZZ (WZ) production in proton–proton collisions with integrated luminosities of 1.3 fb^{-1} at $\sqrt{s} = 13$ TeV using the $ZZ \to \ell\ell\ell'\ell'(WZ \to \ell\nu\ell'\ell')$ decays ($\ell = e, \mu$), recorded with the CMS detector in 2015 [6, 7].

The measured yields are used to evaluate the ZZ (WZ) production cross section in the fiducial phase space which is defined by several kinematics cuts on leptons. To obtain the total ZZ (WZ) cross section, the measured fiducial cross section is corrected for: *(i)* the acceptance of the fiducial selections, estimated from simulation and *(ii)* for Z and W leptonic branching fractions. The $Z \to \ell\ell$ branching fraction is taken to

be 3.37%. For W, the average branching fraction to leptons is $(10.67 \pm 0.16)\%$, for the electron channel $(10.71 \pm 0.16)\%$ and for the muon channel $(10.63 \pm 0.15)\%$. The total ZZ and WZ production cross section is measured to be $16.7^{+2.9}_{-2.6}(\text{stat.})^{+0.7}_{-0.5}(\text{sys.}) \pm 0.3(\text{theo.}) \pm 0.8(\text{lumi.})$ pb and $36.8 \pm 4.6(\text{stat.})^{+8.1}_{-6.2}(\text{sys.}) \pm 0.6(\text{theo.}) \pm 1.7(\text{lumi.})$ pb respectively. The measured total cross sections can be compared to the theoretical values of ZZ and WZ $16.5^{+0.7}_{-0.5}$ pb and $42.7^{+1.6}_{-0.8}$ pb respectively, calculated using NNPDF3.0 PDF an renormalization and factorization scale $\mu_{\mathrm{R}} = \mu_{\mathrm{F}} = M_{Z(W)}/2$. Measurements are found to be consistent with theoretical predictions.

4.3. Inclusive jet production

A measurement of the double-differential inclusive jet cross section, as a function of jet transverse momentum p_{T} and jet rapidity $|y|$, has also been made by using CMS recorded data of proton–proton collisions [8]. The collected data correspond to an integrated luminosity of 72 pb^{-1} for rapidities up to $|y| = 3$ and 45 pb^{-1} for the forward rapidity region $3.2 < |y| < 4.7$. The result covers a large range in jet p_{T} from 114 GeV up to 2 TeV, in six rapidity bins starting from $|y| = 0$ up to $|y| = 3$ with $|\Delta y| = 0.5$, and one bin from $|y| = 3.2$ to $|y| = 4.7$ corresponding to the forward rapidity region shown in Fig. 6. The measurement has been performed for two different jet cone radii $R = 0.4$ and 0.7 for the anti-k_{T} jet algorithm.

By comparing the data to predictions at NLO accuracy in pQCD, it is observed that jet cross sections for the larger jet size of $R = 0.7$ are better described than for $R = 0.4$. In contrast, NLO predictions matched to parton showers from POWHEG + PYTHIA 8, even with two different tunes, perform equally well for both jet size parameters as the fixed-order prediction for the larger jet size of $R = 0.7$. This is in agreement with the measurement performed at the center-of-mass energy of 7 TeV, where it was observed that POWHEG + PYTHIA 8 correctly describes the R dependence of the inclusive jet cross section, while fixed-order predictions at NLO fail in that respect. Predictions by the LO MC generators PYTHIA 8 and HERWIG++ exhibit significant discrepancies with respect to data. The discrepancies are more pronounced in the case of HERWIG++.

4.4. Z+jets differential cross sections

Differential cross-section measurements of the $Z(\rightarrow \mu\mu)$ boson production in association with jets are presented, using 13 TeV proton–proton collisions data recorded by the CMS detector at the LHC, corresponding to an integrated luminosity of 2.5 fb^{-1} [9]. The cross sections are presented as a function of jet multiplicity, the jet transverse momenta, and the jet rapid-

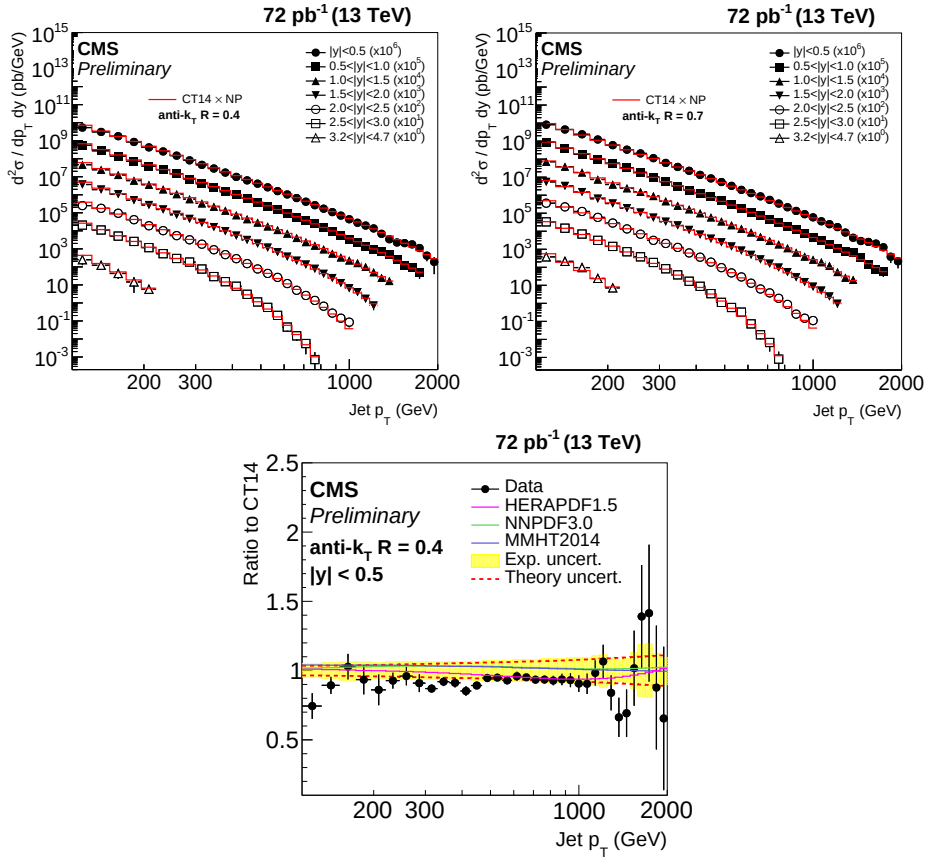

Fig. 6. Measured cross section as a function of the inclusive jets multiplicity (top) and as a function of the p_{T} of the first jet (bottom).

ity for different jet multiplicities. The cross-section measurements are then compared with the predictions from a multileg next-to-leading-order Monte Carlo generator.

Figure 7 (left) shows the measured cross section as a function of the inclusive jets multiplicity. Good agreement between reconstructed data and simulation is observed up to four jets. Good agreement is to be expected up to three jets since the used MG5_aMC@NLO sample describes up to two partons at NLO, with different multiplicities merged and matched with parton shower, not a fixed multiplicity. Above a multiplicity of three, the jets are simulated only by the parton shower of PYTHIA 8. Figure 7 (right) shows the measured cross section as a function of the transverse momentum of the leading p_{T} jets. All data distributions are well-reproduced by the simulation, although the third jet p_{T} is decreasing a little more rapidly in data than simulation.

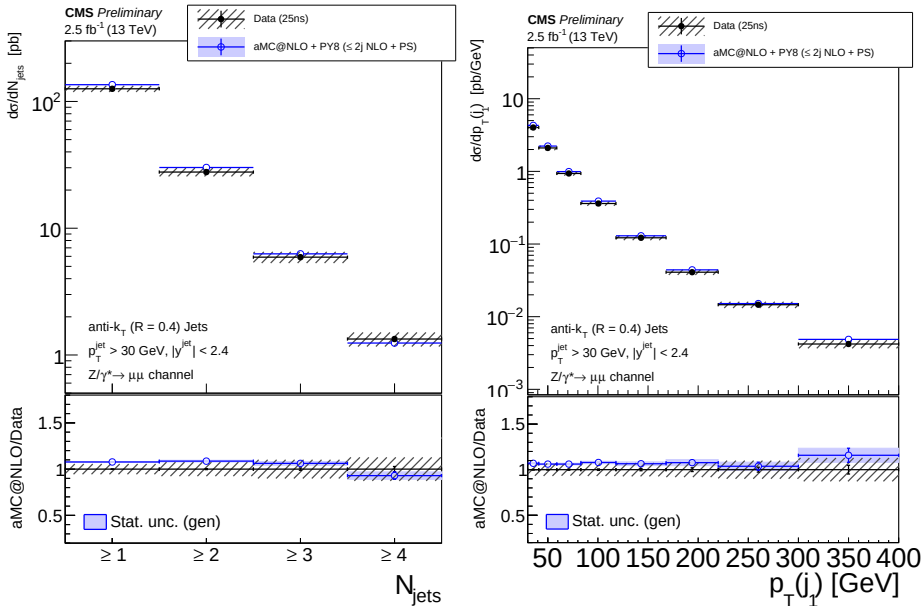

Fig. 7. Measured cross section as a function of the inclusive jets multiplicity (left) and as a function of the p_{T} of the first jet (right).

5. Top physics results

5.1. Inclusive and differential $t\bar{t}$ cross section

The CMS experiment also reported top–antitop quark ($t\bar{t}$) production measurement in proton–proton collisions at $\sqrt{s} = 13$ TeV at the CERN LHC, using data corresponding to an integrated luminosity of 42 pb^{-1} in the dilepton decay channels ($e^+e^-, \mu^+\mu^-, \mu^\pm e^\pm$), ℓ + jets decay channels ($\ell = e, \mu$) and $e\mu$ decay channel [10–13]. The $t\bar{t}$ production cross section is measured as a function of kinematic properties, invariant mass, event variables of the top-quark and $t\bar{t}$ system. The results are compared with predictions from different Monte Carlo event generators, which are all able to describe the data within their large statistical uncertainties. Few selected results are shown in Figs. 8–11.

5.2. t-channel single top production

A measurement of the t-channel single top-quark cross section is also performed using 42 pb^{-1} proton–proton collisions data at 13 TeV with one muon in the final state [14]. The signal is extracted from a fit to the pseudorapidity distribution of the recoiling jet. The inclusive cross section is measured to be $\sigma_{t\text{-ch}} = 274 \pm 98(\text{stat.}) \pm 52(\text{syst.}) \pm 33(\text{lumi.})$. The observed

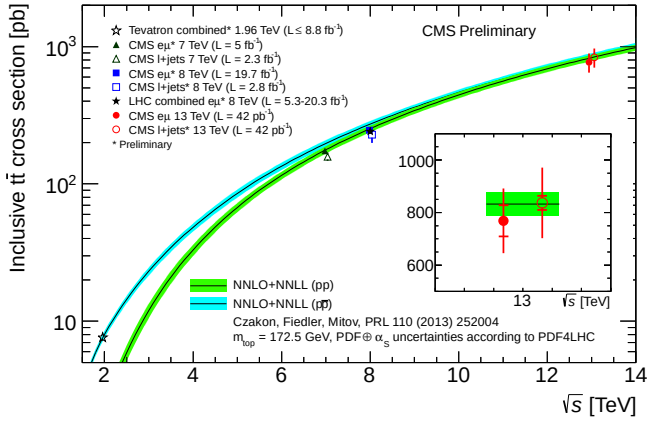

Fig. 8. Top-quark pair cross-section summary of most precise CMS measurements in the dilepton and ℓ + jets channel in comparison with the theory calculation at NNLO+NNLL accuracy. The Tevatron measurements are also shown.

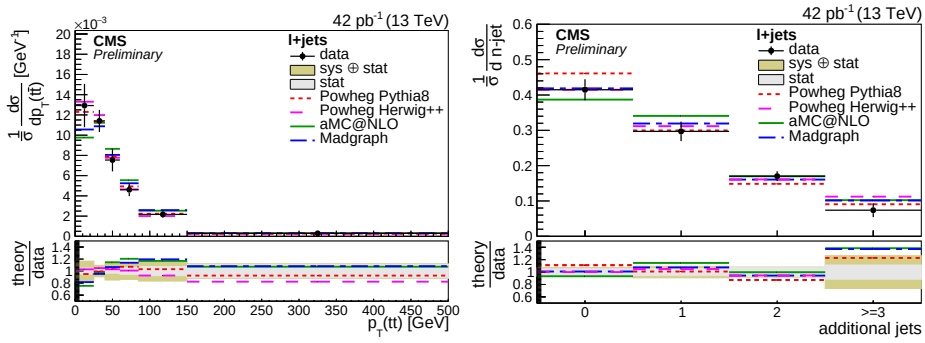

Fig. 9. Normalized differential cross sections as a function of $p_{(t\bar{t})}$ (left) and jet multiplicity (right) compared to the predictions of POWHEG + PYTHIA 8, POWHEG+HERWIG++, MG5_aMC@NLO+PYTHIA 8, and MadGraph+PYTHIA 8.

(expected) significance of the signal contribution is 3.5 (2.7) standard deviations with respect to the background-only hypothesis. The results are found to be in agreement with Standard Model predictions as shown in Fig. 12.

5.3. Underlying event studies in $t\bar{t}$ events

Measurements of the underlying event (UE) activity using charged particle properties in $t\bar{t}$ events in the μ + jets channel are presented [15] using 2.2 fb^{-1} proton–proton collision at 13 TeV data. Selected results are shown in Fig. 13. The measurements are found to be consistent with the predictions from the QCD Monte Carlo model generators used by CMS for the LHC Run 2 data.

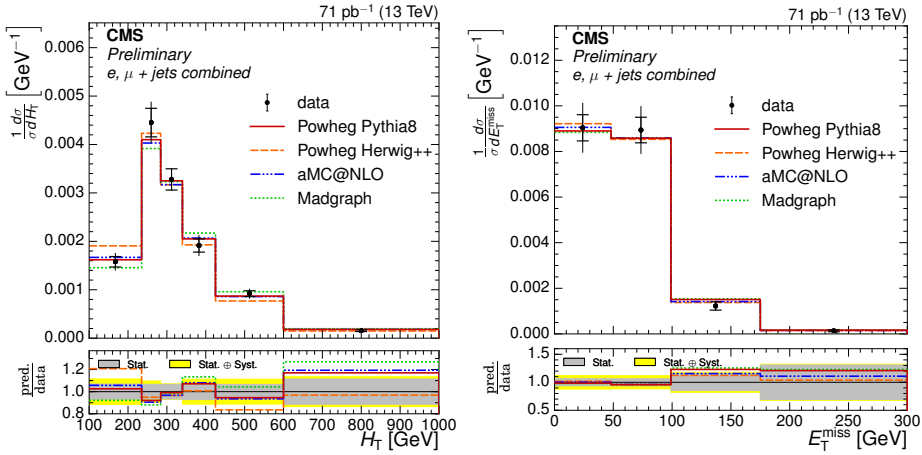

Fig. 10. Comparison of measured normalised differential cross section with respect to H_{T} (left) and $E^{\mathrm{T}}_{\mathrm{miss}}$ (right) to different event generators (a) and MC tunes (b) for the combined channel at a center-of-mass energy of 13 TeV. The inner vertical bars denote the statistical uncertainty, and the outer bar denotes the total uncertainty.

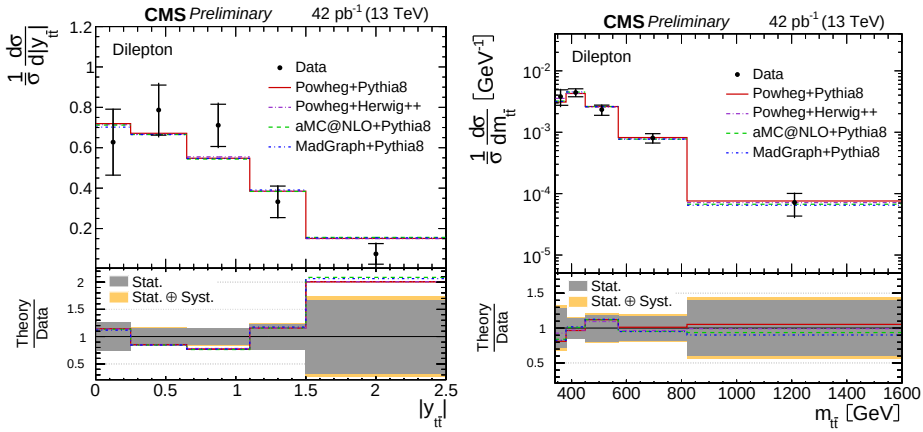

Fig. 11. Normalized differential $t\bar{t}$ production cross section as a function of the $|y_{t\bar{t}}|$ (left) and $m_{t\bar{t}}$ (right) of the top-quark pairs. The inner (outer) error bars indicate the statistical (combined statistical and systematic) uncertainty. The measurements are compared to predictions from: POWHEG + PYTHIA 8, MG5_aMC@NLO + PYTHIA 8, MadGraph + PYTHIA 8, and POWHEG + HERWIG++.

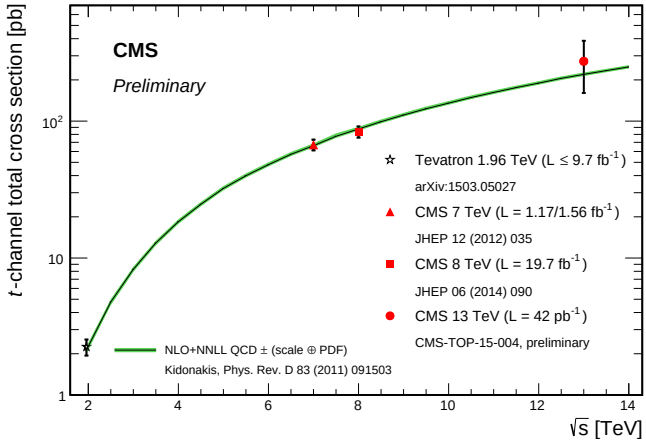

Fig. 12. Summary of t-channel single top cross-section measurements by CMS, as a function of center-of-mass energy.

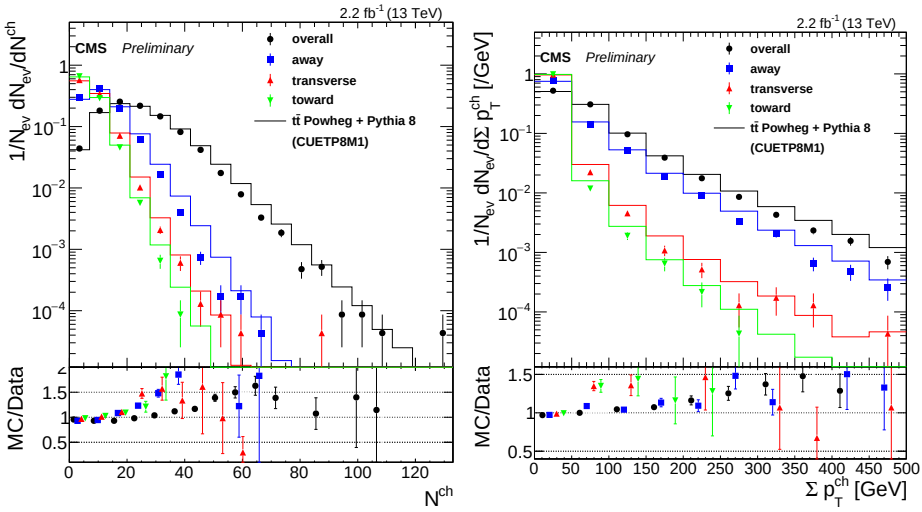

Fig. 13. The charged PF candidate multiplicity (left) and transverse momentum sum (right) distributions for the away, transverse and toward regions as well as for the overall sample. Distributions are obtained with the nominal Q^2 scale. The points correspond to the data at the detector level and the lines represent the POWHEG + PYTHIA 8 predictions with the CUETP8M1 tune. In this figure, each distribution is normalized to one.

6. Conclusions

After a very successful Run 1 of the LHC, marked by the discovery of a Higgs boson with a mass of approximately 125 GeV, CMS made several Standard Model physics measurement using the LHC Run 2 proton–proton collision at 13 TeV data corresponding to integrated luminosity up to 2.5 fb^{-1}. Figure 14 shows summary of cross-section measurements and corresponding theoretical predictions made by CMS using data of 7, 8 and 13 TeV data. Run 2 measurements uncertainties are dominated by luminosity uncertainty. All of the results are found to be consistent with the SM predictions. The Standard Model will be tested with an unprecedented level of precision in new unexplored territories during the Run 2, setting as well the ground for new physics.

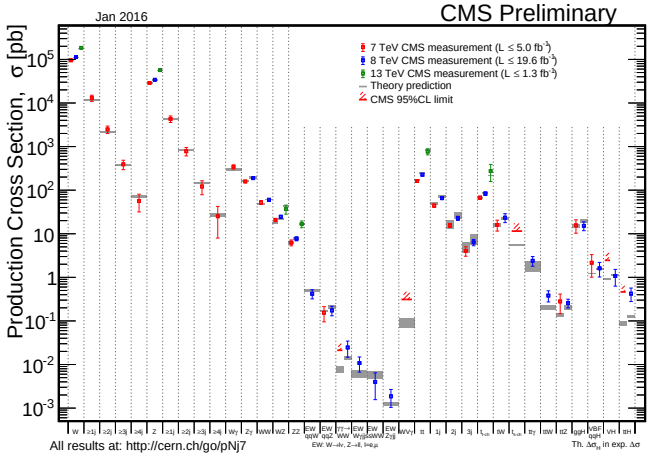

Fig. 14. Summary of CMS cross-section measurements.

REFERENCES

[1] CMS Collaboration, *Phys. Lett. B* **751**, 143 (2015).

[2] CMS Collaboration, *Phys. Rev. Lett.* **116**, 172302 (2016).

[3] CMS Collaboration, Underlying Event Measurements with Leading Particles and Jets in *pp* Collisions at $\sqrt{s} = 13$ TeV, CMS Physics Analysis Summary CMS PAS FSQ-15-007, 2015.

[4] CMS Collaboration, Measurement of the B^+ Hadron Production Cross Section in *pp* Collisions at 13 TeV, CMS Physics Analysis Summary CMS PAS BPH-15-004, 2015.

[5] CMS Collaboration, Measurement of Inclusive W and Z Boson Production Cross Sections in pp Collisions at $\sqrt{s} = 13$ TeV, CMS Physics Analysis Summary CMS PAS SMP-15-004, 2015.

[6] CMS Collaboration, Measurement of the ZZ Production Cross Section in $\ell\ell\ell'\ell'$ Decays in pp Collisions at $\sqrt{s} = 13$ TeV, CMS Physics Analysis Summary CMS PAS SMP-15-005, 2015.

[7] CMS Collaboration, Measurement of the WZ Production Cross Section in pp Collisions at $\sqrt{s} = 13$ TeV, CMS Physics Analysis Summary CMS PAS SMP-15-006, 2015.

[8] CMS Collaboration, Measurement of the Double-differential Inclusive Jet Cross Section at $\sqrt{s} = 13$ TeV, CMS Physics Analysis Summary CMS PAS SMP-15-007, 2015.

[9] CMS Collaboration, Measurement of the Differential Cross Section of Z Boson Production in Association with Jets in Proton–Proton Collisions at $\sqrt{s} = 13$ TeV, CMS Physics Analysis Summary CMS PAS SMP-15-010, 2015.

[10] CMS Collaboration, *Phys. Rev. Lett.* **116**, 052002 (2016).

[11] CMS Collaboration, Measurement of the Inclusive and Differential $t\bar{t}$ Production Cross Sections in Lepton+Jets Final States at 13 TeV, CMS Physics Analysis Summary CMS PAS TOP-15-005, 2015.

[12] CMS Collaboration, First Measurement of the Differential Cross Section for $t\bar{t}$ Production in the Dilepton Final State at $\sqrt{s} = 13$ TeV, CMS Physics Analysis Summary CMS PAS TOP-15-010, 2015.

[13] CMS Collaboration, Measurement of Differential Top Quark Pair Production Cross Sections in a Fiducial Volume as a Function of Event Variables in pp Collisions at $\sqrt{s} = 13$ TeV, CMS Physics Analysis Summary CMS PAS TOP-15-013, 2015.

[14] CMS Collaboration, Measurement of the tt-channel Single Top-quark Cross Section at 13 TeV, CMS Physics Analysis Summary CMS PAS TOP-15-004, 2015.

[15] CMS Collaboration, Underlying Event Measurement with $t\bar{t} + X$ Events with pp Collision data at $\sqrt{s} = 13$ TeV, CMS Physics Analysis Summary CMS PAS TOP-15-017, 2015.